JOURNAL OF SOLID STATE CHEMISTRY 106, 134–143 (1993)

HREM Study of the La/K Ordering in Superconducting $La_{2-x}K_xCuO_4$ ($x = .22$ and $x = .27$)

M. A. SEÑARÍS-RODRÍGUEZ AND M. A. ALARIO-FRANCO*

Departamento de Química Inorgánica, Facultad de Ciencias Químicas, Universidad Complutense, 28040 Madrid, Spain

Received December 4, 1992; accepted December 23, 1992

IN HONOR OF SIR JOHN MEURIG THOMAS ON HIS 60TH BIRTHDAY

Electron diffraction and high resolution electron microscopy studies on $La_{2-x}K_xCuO_4$ superconducting samples ($x = .22$ and $x = .27$) reveal that the microstructure of these materials is very complex due to a partial ordering between the La and K cations. This ordering presents different characteristics along each of the three space directions: it is long range in two directions, and along one of these (the [001]) it is incommensurably modulated; in the third direction it is short range, with a coherence length of ≈23–40 Å. © 1993 Academic Press, Inc.

Introduction

Our previous work (*1*) on the potassium doped superconducting sample $La_{1.78}K_{.22}CuO_{4-y}$ has revealed that the microstructure of this material is very complex:

—The distribution of K within the microcrystals is not homogeneous.

—Its structure is not strictly tetragonal.

—It presents modulated structures based on a La_2CuO_4 subcell, whose existence was detected by the presence of extra satellites in the electron diffraction patterns containing the **c*** axis, and the appearance of fringes of different widths in the corresponding low resolution electron micrographs. Very interestingly, the origin of these modulated structures is likely to be related to both the degree of potassium doping and the precise distribution of this cation within each of the microcrystals (*1*).

We present in this paper the results of further studies performed by means of electron diffraction and high resolution electron microscopy on this same $La_{1.78}K_{.22}CuO_{4-y}$ sample and on the also superconducting material $La_{1.73}K_{.27}CuO_{4-y}$.

This work follows from early, indeed pioneering work, by Professor J. M. Thomas on the detailed characterization of real solids and their defects by transmission electron microscopy and electron diffraction.

Experimental

Samples of average composition $La_{2-x}K_xCuO_{4-y}$, with $x = .22$ and $x = .27$, were synthesized from stoichiometric amounts of La_2O_3 and CuO by direct precipitation from molten KOH. Details of the procedure are indicated in (*2*).

Specimens for transmission electron microscopy were prepared by grinding them, dispersing them in propanol, and putting a few droplets on a copper grid. Electron diffraction and X-ray microanalysis were carried out in a JEOL 2000 FX microscope, working at 200 kV. High resolution electron

* To whom correspondence should be addressed.

0022-4596/93 $5.00

microscopy was performed on a JEOL 4000 EX instrument, with a CS = 1.0 nm, operating at 400 kV.

Simulated images were obtained using the NCEMSS program, run on a VAX station.

Electron Diffraction Results

The electron diffraction studies show that there are no significant differences between thes two samples ($x = .22$ and $x = .27$). So we describe them on a common basis, just remarking some minor particular features.

As we had already observed for the case of $La_{1.78}K_{.22}CuO_{4-y}$ (*1*), these materials are neither monophasic nor strictly tetragonal. Also, most of the crystals belonging either to the $La_{1.78}K_{.22}CuO_{4-y}$ sample or to the $La_{1.78}K_{.27}CuO_{4-y}$ sample give rise to [*hk*0] electron diffraction patterns which present *two* types of diffraction maxima (Fig. 1):

—Strong spots, which can be approximately indexed on the basis of a pseudotetragonal La_2CuO_4 type cell, with space group *I*4/*mmm* (allowed "reflections": *hkl*: $h + k + l = 2n$; *hk*0: $h + k = 2n$; *hhl*: $l = 2n$; 0*kl*: $k + l = 2n$; 00*l*: $l = 2n$) and parameters **a** = 3.77 Å, **c** = 13.3 Å).

It is worth mentioning that while in the case of the $La_{1.73}K_{.27}CuO_{4-y}$ sample the angle between $\mathbf{g}_{001}$ and all the directions contained in the basal reciprocal plane is 90°, in the case of microcrystals of the sample with average composition $La_{1.78}K_{.22}CuO_{4-y}$ that angle has a value varying between 88° and 89°, suggesting a slight monoclinic distortion.

—Extra reflections, of weaker intensity, appearing on both sides of the allowed reflections along **c*** (although in the case of the sample of $La_{1.78}K_{.22}CuO_{4-y}$ these satellite reflections appear slightly off but still rather close to that direction). These are the first order satellites of the main reflections, whose presence suggests the existence of a modulated structure.

The period of the modulation, d^*_{sat}, which is observed to change from crystal to crystal even in the same sample (see for example Figs. 3 and 4 in (*1*)), takes the values indicated in Table I. It can be observed from that table that none of these distances is an integral multiple of the **c** axis, which means

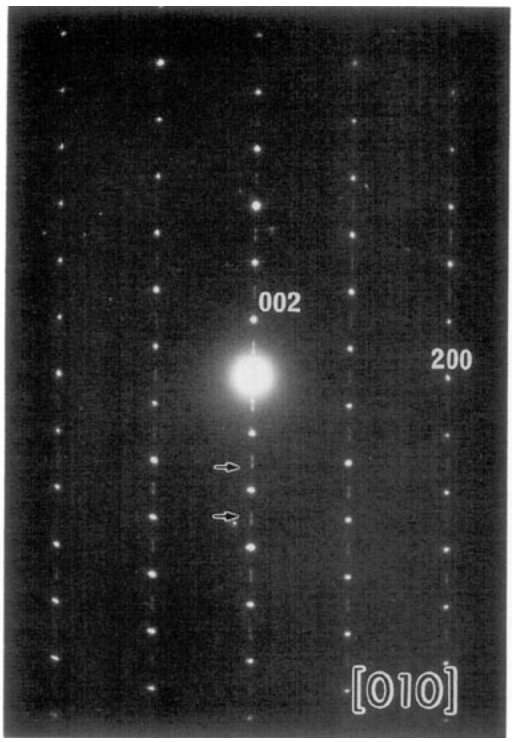

FIG. 1. Typical [010] electron diffraction pattern of potassium-doped microcrystals. For this particular case, the modulation shows a periodicity of 1/15.69 $Å^{-1}$.

TABLE I

SEPARATION BETWEEN MAIN SPOT AND ITS SATELLITES, OBTAINED FROM DIFFERENT MICROCRYSTALS

d(A)	d/c
15.69	1.18
16.36	1.26
17.42	1.31
19.99	1.50

Note. In column 1 of this table, periodicity has been expressed as absolute real values, and in column 2 as relative values referred to **c** units (**c** = 13.3 Å, as deduced from X-ray diffraction results).

that these modulations are incommensurate relative to the basic La_2CuO_4 type cell.

Another interesting information is obtained when, starting from the (**ac**)* plane, we tilt around the **a*** axis. In this case, over a tilt angle which, depending on the crystal, varies between $\pm 13°$ and $\pm 19°$, those satellite reflections remain visible. On tilting further, and going through the zone axes $[06\bar{1}]$, $[05\bar{1}]$, and $[04\bar{1}]$ (Figs. 2a, 2b, and 2c), very faint extra spots appear next to reflections which are, in principle, forbidden in SG *I4/mmm*. These extra spots are no longer visible on the $[03\bar{1}]$ zone axis.

These results indicate that the satellites present in the reciprocal space lattice are not spherical as we had previously thought (*1*), but rodlike; their length, although variable from crystal to crystal, is typically $(4.35–2.5) \times 10^{-2}$ Å^{-1}, which corresponds to 23–40 Å in real units. These rods are situated perpendicular to the **c*** axis, and their separation from the corresponding main spots depends on the crystal.

Their orientation on the reciprocal plane parallel to (**ab**)* has not yet been obtained by means of electron diffraction. The best, and perhaps the only way to determine this is through long exposure precession experiments in a plane parallel to (**ab**)* and at a distant d^*_{sat} from it (*3*). Yet the inhomogeneous compositional distribution observed from crystal to crystal, and even from region to region within a given crystal, as suggested by the fluctuations in the modulation length, Table I, may hamper or even prevent its successful determination.

In any case, with the ensemble of the results obtained by electron diffraction, we can postulate a more elaborated and complex model for the reciprocal lattice of these crystals (Fig. 3).

According to this model, the extra reflections appearing on zone axes $[06\bar{1}]$, $[05\bar{1}]$, and $[04\bar{1}]$ arise from the intersection of the reciprocal plane (in fact, the Ewald sphere) and the rods around the main spots situated just above and below these weak reflections (Fig. 4).

Interpretation of the Reciprocal Lattice

The fact that first order satellites are the only ones visible seems to suggest that modulation is compositional and not displacive. According to Buseck and Cowley (*4*), in compositional modulations, i.e., when the occupation factor of the atomic positions is modulated, the intensity of the satellites decreases from the first satellite as the separation from the main spot increases, so that second and higher order satellites are often invisible. On the other hand, in the case of modulated displacements the satellite intensity has a maximum at a higher order harmonic.

In view of the composition of the present samples, it appears likely that this modulation is related to an imperfect K/La ordering. Moreover, the fact that only first order satellites are present is a strong indication of a sinusoidal modulation (*5*).

On the other hand, taking into account that the correlation length along one direction is inversely proportional to the length of the satellite along that direction, the rodlike nature of these satellites indicates that the modulation has a different coherence length in the three dimensions. It is long range along [001] (along which it is incommensurately modulated) and along $[-\sin\alpha, -\cos\alpha, 0]$. But it is only moderately short range in the direction corresponding to the rod-length, i.e., $[-\cos\alpha, \sin\alpha, 0]$ (α being the angle between the projection of the rod on the **a***b*** plane and the **b*** axis); as indicated above, this length varies between $\simeq$23 and 40 Å.

High Resolution Electron Microscopy Results

I. La_2CuO_4 Microcrystals

The first crystals studied were those which, although belonging to these $La_{2-x}K_xCuO_4$ samples, did not show satellite reflections in the electron diffraction patterns containing the **c*** axis. These crystals were presumed to be potassium-free, as was sub-

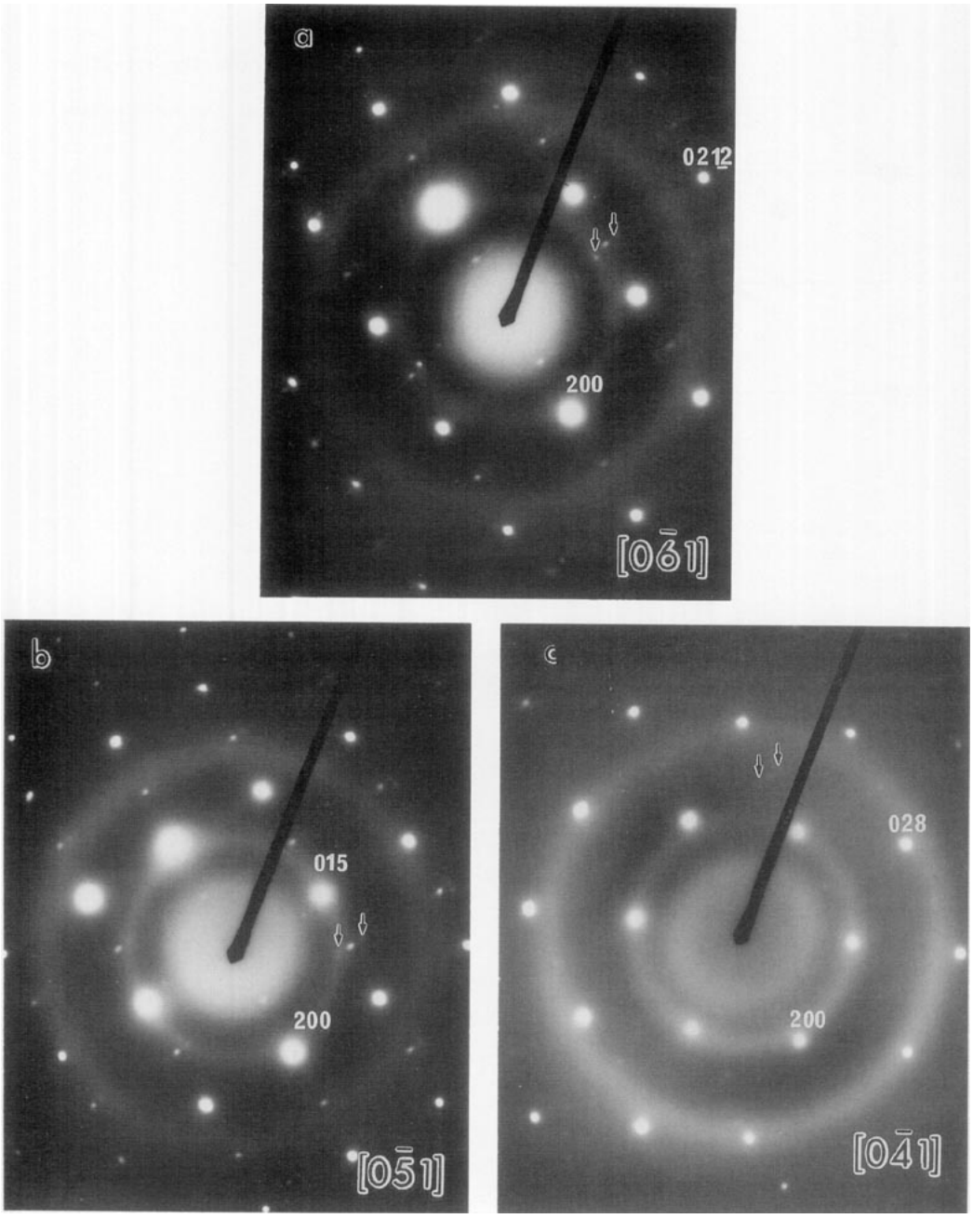

Fig. 2. ED patterns of these $La_{2-x}K_xCuO_{4-y}$ samples, $x = .22$ and $x = .27$, along the following zone axes: (a) $[06\bar{1}]$, (b) $[05\bar{1}]$, and (c) $[04\bar{1}]$. Very faint extra spots around "forbidden reflections" are marked by arrows.

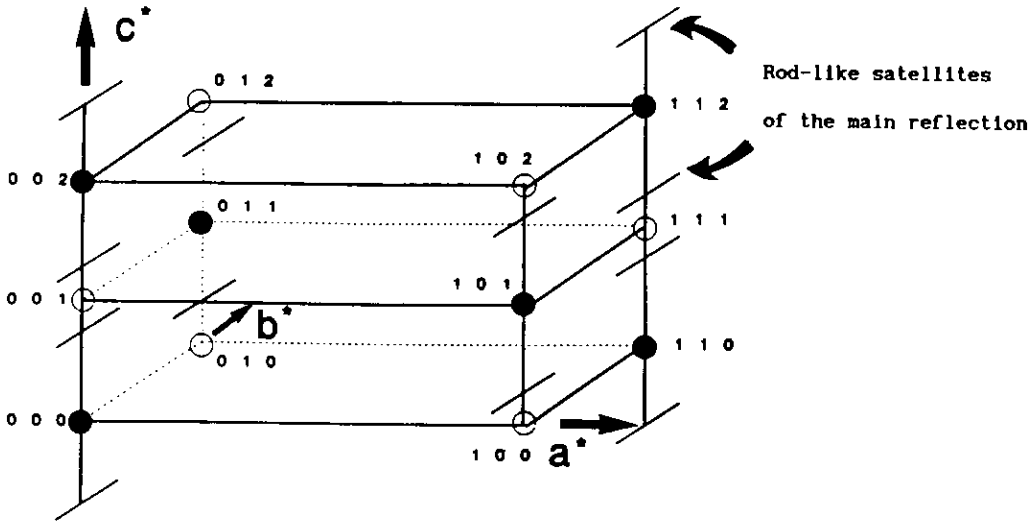

FIG. 3. Perspective drawing of the reciprocal lattice for $La_{2-x}K_xCuO_{4-y}$, $x = .22$ and $x = .27$. The length of the satellites is out of scale to show more clearly their presence. (●) Allowed reflection of a tetragonal La_2CuO_4-type cell (SG *I4/mmm*); (○) extinction; (—) rod-like satellite.

sequently confirmed by X-ray microanalysis.

In the corresponding HREM images, the contrast observed is that expected for a La_2CuO_4 structure. For example, Fig. 5 shows an underfocus image of these microcrystals taken along the direction $[110]_o$ ($\langle\ \rangle$ $[100]_t$); this is a particularly interesting orientation since, along it, each atomic column consists of a single type of atoms, so that the layer sequence along **c** is

$$\ldots -CuO_2—LaO—LaO–CuO_2–$$
$$LaO–LaO–CuO_2- \ldots$$

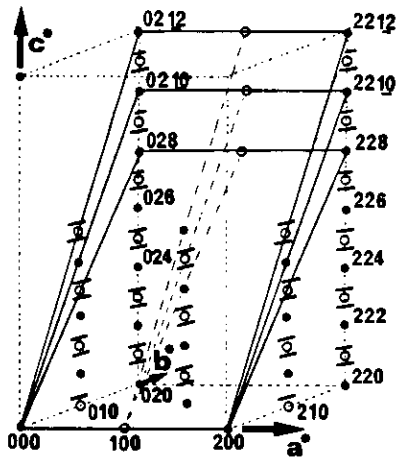

FIG. 4. Schematic drawing of the tilting around **a***, so as to detect the rod-like nature of the satellites (cf. Fig. 2).

II. $La_{2-x}K_xCuO_4$ Microcrystals

Images of the doped crystals are indeed very different from those of the pure material. However, as the micrographs of samples with $x = .22$ or $x = .27$ are basically similar, we describe them on a common basis.

As already detected by low and medium resolution electron microscopy (*1*), the HREM pictures (Figs. 6 and 7) show marked changes in contrast along **c**, as well as along the perpendicular to that direction (the [100] in Figs. 6 and 7). Also, one can distinguish an undulation of the [100] planes (Fig. 7).

And as is evident from such images, where the contrast varies very quickly from region to region, in these potassium-doped microcrystals the situation is very inhomogeneous, even on a local scale. So, in order to understand this peculiar microstructure,

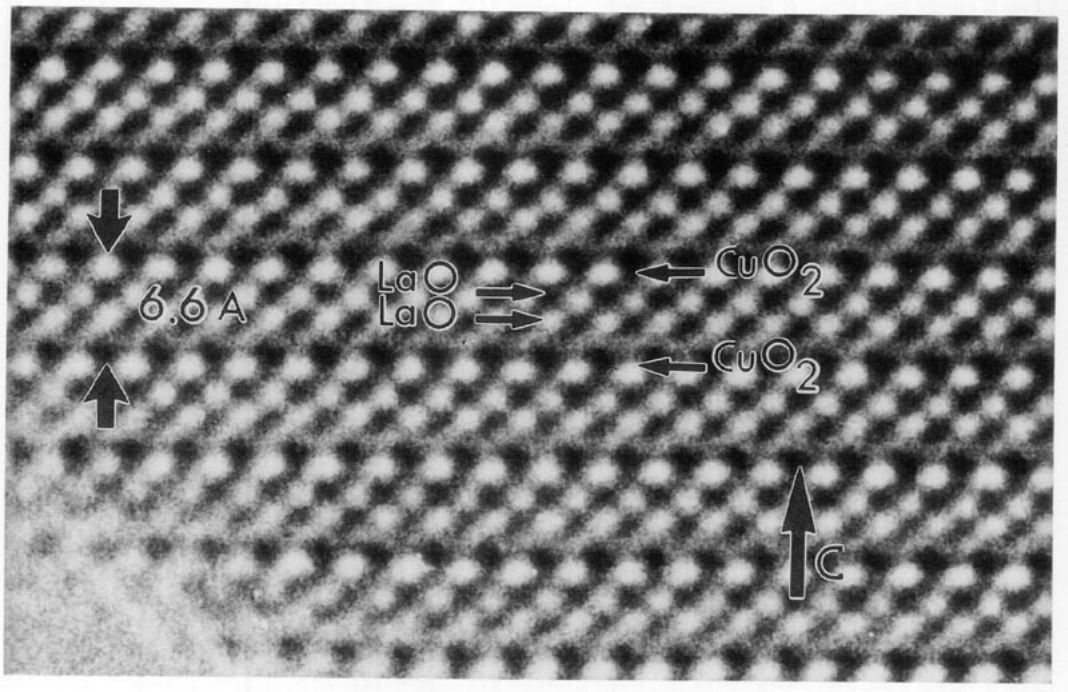

FIG. 5. Underfocus high resolution electron image, showing a "normal", i.e., undoped La_2CuO_4 structure. Zone axis $[110]_0 \langle\rangle [010]_t$.

we try to describe the situation present in one small zone, such as that displayed in Fig. 8; nevertheless, the procedure that we follow can be equally applied to any other region of any other crystal.

In the photograph in Fig. 8, it can be clearly seen that the two (LaO) type planes between the CuO planes show a markedly different contrast, one being much brighter and resembling the adjacent CuO_2 plane.

Now, considering

(a) previous single crystal X-ray diffraction studies performed on similar potassium-doped samples that show some ordering between La^{3+} and K^+ (*6*);

(b) the incommensurate compositional modulation detected by means of electron diffraction;

(c) the [001] interplanar separation of 6.65 Å present in the HREM mirographs, corresponding to the d_{002} of the La_2CuO_4 basic subcell; and

(d) the big difference in the electron scattering factors of La^{3+} and K^+ (*7*),

it is reasonable to assign those differences in the contrast of the (LaO) type planes to a partial substitution of La^{3+} by K^+ in the basic La_2CuO_4 type cell.

Obviously there are many possible sequences in such substitution and the problem becomes even more acute if one introduces partial ordering in other directions within the (K/La)O plane. For these reasons we did assume, in a first approximation, that there was no extra ordering on that plane so that, in the [010] projections (corresponding to Figs. 6–8), along an atomic row parallel to **b**, all atoms are alike, i.e., all are La or K or Cu.

On this basis, the following sequences were simulated (Fig. 9):

$-CuO_2-LaO-LaO-CuO_2-LaO-KO-CuO_2-$

$-CuO_2-LaO-LaO-CuO_2-KO-KO-CuO_2-$

$-CuO_2-LaO-KO-CuO_2-KO-LaO-CuO_2-$

$-CuO_2-LaO-KO-CuO_2-LaO-KO-CuO_2-$

In any of these simulated models, it became

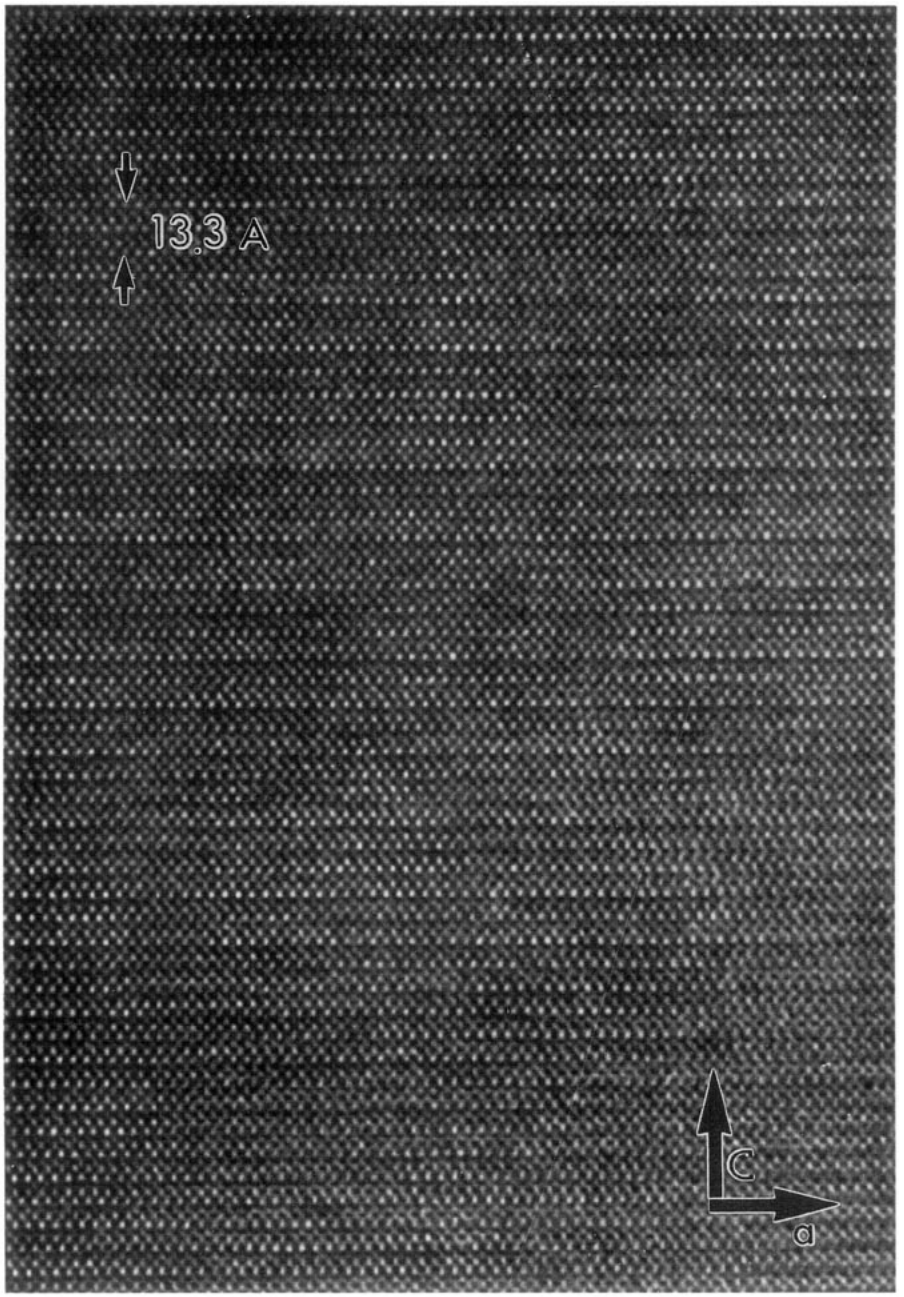

FIG. 6. Typical high resolution electron micrograph of a potassium-doped microcrystal. It shows marked variations in contrast, along both **c** and **a**.

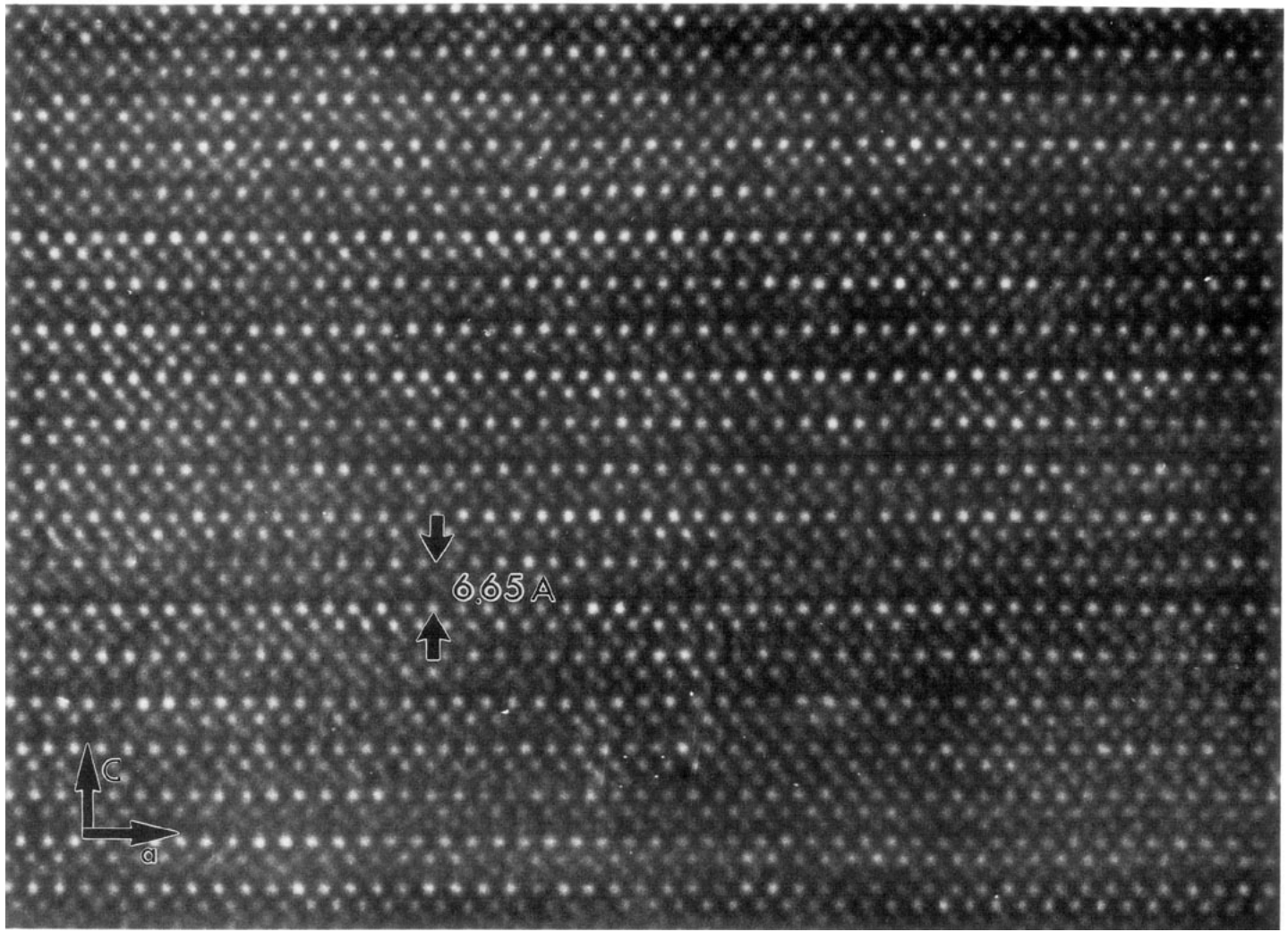

FIG. 7. HREM of these $La_{2-x}K_xCuO_{4-y}$, at higher magnification. In addition to evident contrast changes, undulations of the CuO planes are also visible. These are better seen by observing the picture at a glazing angle along the [100] direction.

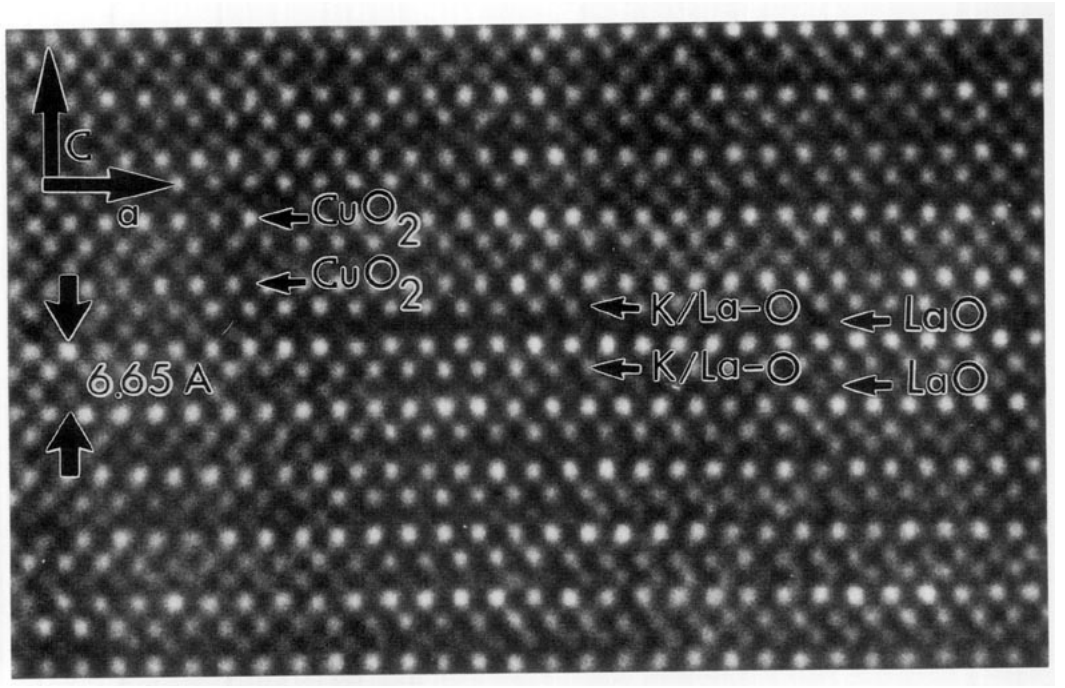

FIG. 8. Small zone of Fig. 7, in which the contrast of the two LaO-type planes between the CuO planes is alternatively bright and dark (cf. Fig. 5).

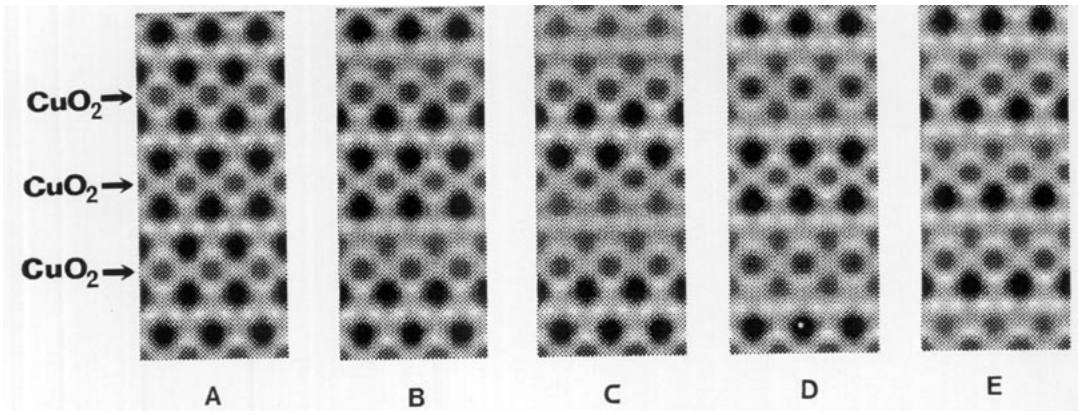

FIG. 9. Simulated images corresponding to the following stacking sequences: (A) . . . $-CuO_2-LaO-LaO-CuO_2-LaO-LaO-CuO_2-$ . . . , (B) . . . $-CuO_2-LaO-LaO-CuO_2-LaO-KO-CuO_2-$ . . . , (C) . . . $-CuO_2-LaO-LaO-CuO_2-KO-KO-CuO_2-$ . . . , (D) . . . $-CuO_2-LaO-KO-CuO_2-KO-LaO-CuO_2-$ . . . , (E) . . . $-CuO_2-LaO-KO-CuO_2-LaO-KO-CuO_2-$ . . . . They correspond to the [010] zone axis and have been obtained for a defocus value (Δf) of -450 Å (approx. Scherzer focus) and a crystal thickness (t) of 15 Å.

obvious that a KO plane has a very different contrast from that of a pure LaO plane, but is very similar to that of a CuO_2 plane.

A comparison between through focus simulated images, for different crystal thickness values, and the experimental pictures indicates that the last sequence, in which a KO plane substitutes every other LaO plane, gives the best fit. According to the simulation, while the "LaO"-type planes with a darker contrast will contain only La^{3+} cations, those with brighter contrast should correspond to lattice planes where La^{3+} positions have been occupied by K^+ cations. In fact, these are indeed larger ($^{IX}r_{K^+} = 1.55$ Å and $^{IX}r_{La^{3+}} = 1.22$ Å (*8*)), but have a much smaller scattering power which, in turn, is rather similar to that of the Cu.

It is also worth noting that substitution of La^{3+} by K^+ in those planes is nevertheless limited, as no pure KO planes are observed, but only mixed (La/K)O planes (cf. the contrast change along [100] in Figs. 6–8).

Consequently, the stacking sequence along **c** in that zone can be represented as

. . . –CuO–LaO–(K/La)O–CuO–LaO–
(K/La)O–CuO– . . . .

There are a number of interesting points that this sequence suggests. First of all is the fact that K^+ and La^{3+} get ordered. This is no doubt due to the combined contributions of very different charges and radii (cf. $^{IX}r_{K^+} = 1.55$ Å and $^{IX}r_{La^{3+}} = 1.22$ Å). This is sometimes referred to as ionic potential (q/r). In this case $(q/r)_{K^+} = .625$ and $(q/r)_{La^{3+}} = 2.647$, a strong driving force for the ordering!. However, we have never observed in the present crystals two consecutive "KO planes"; i.e., the La ions are only substituted by K in every other plane, and this only partly. This sounds reasonable since a sequence such as

. . . –CuO–KO–KO–CuO . . .

implies the totally unreasonable composition "K_2CuO_4." On the same basis, it is not unexpected to observe that there are no KO-only planes, but always mixed (K/La)O planes. Again a composition such as "$LaKCuO_4$" seems impossible in terms of the oxidation state of copper.

On the other hand, the amount of potassium that enters in every other (LaO)-type plane is not constant but sinusoidally modulated along **c**, as deduced from ED results. The incommensurate periodicity of this modulation changes from crystal to crystal, and as shown by X-ray microanalysis it depends on the total amount of potassium present: the bigger the doping the smaller the period.

Concerning the observed undulations of the copper–oxygen planes (see for example Fig. 7), they are probably due to a displacement of the cations which move to compensate for the defect of charge introduced by the K doping. This means that the compositional modulation is accompanied by a displacive one, as is normally the case.

Acknowledgments

We thank S. Stoll and A. Stacy, from the College of Chemistry of the University of California at Berkeley, for providing us these samples and for many valuable discussions. We also acknowledge the Centre for Electron Microscopy of our university for technical support. This work has been supported by CICYT (Project MAT 89/0768), EIT, and the MIDAS Superconductivity Program, as well as by Research Awards provided by the "Domingo Martínez" and "Ramón Areces" foundations.

References

1. M. A. Señarís-Rodríguez, M. A. Alario-Franco, S. L. Stoll, and A. Stacy, submitted for publication.
2. S. L. Stoll, Ph.D. Thesis (1992); to be published.
3. M. A. Alario-Franco, I. E. Grey, J. C. Joubert, H. Vincent, and M. Labeau, *Acta Crystallogr. Sect. A* **38,** 117 (1982).
4. P. R. Buseck and J. M. Cowley, *Am. Mineral.* **68,** 18 (1983).
5. A. Guinier in "Théorie et technique de la Radiocristallographie," Chap. XIII, Dunod, Paris (1964).
6. S. Stoll, A. Stacy, and C. C. Torardi, to be submitted.
7. P. A. Doyle and P. S. Turner, *Acta Crystallogr. Sect. A* **24,** 390 (1968).
8. R. D. Shannon and C. T. Prewitt, *Acta Crystallogr. Sect. B* **25,** 925 (1969).